Progress In Electromagnetics Research, Vol. 110, 199–218, 2010

RFID BASED COLLISION-FREE ROBOT DOCKING IN CLUTTERED ENVIRONMENT

M. Kim and K. Kim

Sogang Institute of Advanced Technology, Sogang University
1 Shinsu-dong, Mapo-gu, Seoul, Republic of Korea

N. Chong

School of Information Science
Japan Advanced Institute of Science and Technology
1-1 Asahidai, Nomi, Ishikawa, Japan

Abstract—This paper proposes a radio frequency identification (RFID) based collision-free robot docking in cluttered environment. Physical distance estimation sensors are fused to the developed degree of arrival (DOA) guided robot docking system, and collision-avoidance function is implemented based on the vector field histogram technique. Additionally, new simple but efficient DOA filtering algorithm is developed based on the gain control according to the improved robot control algorithm, which enables the robot to move continuously. The experimental results show that the robot can move to target transponder even though the estimated DOA is blocked by obstacles. The success rate does not reach satisfactory level due to the limitation of the employed sensors and collision-avoidance algorithm, but it is proved that the collision-free docking becomes available without any *priori* map and reference stations.

1. INTRODUCTION

Recent development in auto-ID and networking technologies helps a robot identify unknown neighboring environment then make proper action autonomously by constructing easy-to-understand environment for the robot [1, 2]. Specifically, since RFID can identify plural transponders without the need for the line of sight, it is expected to

Received 16 September 2010, Accepted 5 November 2010, Scheduled 19 November 2010
Corresponding author: Kwangsoo Kim (kimks@sogang.ac.kr).

play an important role as a device for storing and sharing the object's information.

However, as most tasks ask a robot to move to a target position which is not supported by common RFID systems, the functions of the location sensing and docking are required. As a stand-alone solution to autonomous mobile robot real environment identification and docking, the RFID-based DOA guidance system has been developed by the authors [3–5]. Firstly, the single antenna based DOA estimation and target docking system was developed [3]. Secondly, the real time target tracking became available by employing the dual directional antenna [4]. Thirdly, DOA estimation filtering algorithm was developed in order to cope with the RF signal distortion in the cluttered environment based on the geometrical relationship between the robot positions and the estimated directions [5]. However, the robot sometimes fails to dock to the target by colliding an obstacle, which allows the RF signal to pass through but blocks the robot itself. Also, a stop, turn, and move control of robot causes unexpected delay in the robot movement, and the filtering algorithm does not work if there are two or more consecutive large errors in the estimated DOA.

To cope with the problems mentioned above, the developed robot docking system is improved as follows. Firstly, the robot control method is enhanced to facilitate continuous movement. Secondly, the DOA estimation error correction algorithm is incorporated based on the gain control technique according to the robot control algorithm. Finally, sonar sensors are fused to the developed system, and collision-avoidance algorithm is implemented based on the vector field histogram technique for the collision-free robot docking. To verify the proposed system, the simulation using the in-house simulator and real robot experiment are performed. The experimental results show that the robot can dock to the target transponder even though the large error is included in the estimated DOA influenced by the cluttered obstacles. Also, they show that the collision-free robot docking becomes available without any information about the positions of the target, the obstacles, and the robot itself in a *priori* map and additional reference stations.

This paper is organized as follows. The comparison with the related works, the brief introduction of the developed system with the fundamentals of DOA estimation, and the improved robot control method are described in Section 2. The newly developed DOA filtering algorithm is explained in Section 3, followed by the collision-avoidance algorithm using physical distance information in Section 4. Experimental results illustrating the advantages of the developed robot docking system are summarized in Section 5. Finally, conclusions are

drawn in Section 6.

2. DEVELOPED DOA BASED ROBOT DOCKING SYSTEM

2.1. Related Works

Our goal is to develop robot docking system for autonomous mobile robot applications in obstacles cluttered environment. To achieve this goal, vision based approaches have been tried, which help a robot to acquire meaningful information from visual images [6, 7]. However, they require high computing cost and built-in sensors in robot.

Recently, many approaches based on RF communication have been reported [8] such as additional ultrasonic sensor based [9], received signal strength (RSS) based [10], the zone of detected range based [11, 12], and time of arrival (TOA) based [13] systems. However, most of them require multiple reference stations and line of sight for ultrasonic wave transmission. Another approach uses passive RFID array [14], but it requires installation of large number of RFID tags.

In this work, we are interested in DOA (or AOA — angle of arrival) based technique [15], since the direction is very useful information in the target tracking and docking applications. As proposed in this paper, the robot can dock to a target position by following the estimated DOA without any *priori* map or additional sensors. Also, the DOA information can be used to triangulate the target location, if reference stations are provided [16, 17], and relatively accurate location can be estimated in the cluttered environment by fusing other methods such as the distance or the range based techniques to the DOA [18–20].

2.2. Overview of the Developed System

Figure 1 shows the commercial mobile robot customized by the authors to adopt the target docking functionality. The system comprises three parts: 1) the direction-sensing RFID reader employing the dual directional antenna, 2) an off-the-self mobile robot Pioneer 3DX with sonar ring for distance measurement, and 3) the robot controller. An RF module manufactured by Ymatic LTD., Japan is used as both RFID reader and transponder, which operates on 303.2 MHz frequency using 3 V supply.

Figure 2 shows the flowchart of the robot docking in the previous and improved systems. The robot moves to a target transponder by following the estimated DOA until the RSS is over pre-defined value. As the RSS is rapidly increased in near field zone, the robot can recognize the area precisely [3]. The newly added and improved parts

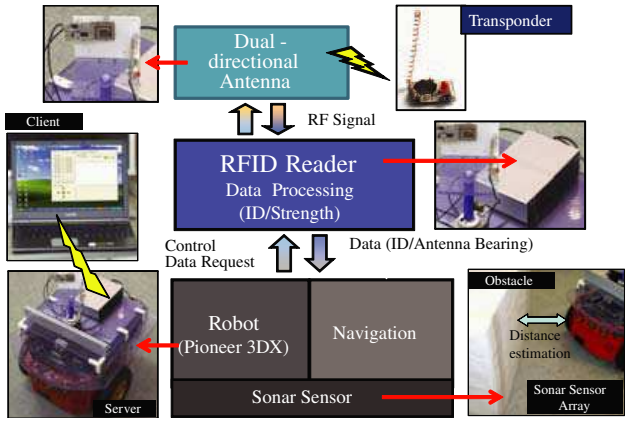

Figure 1. Overview of the developed system.

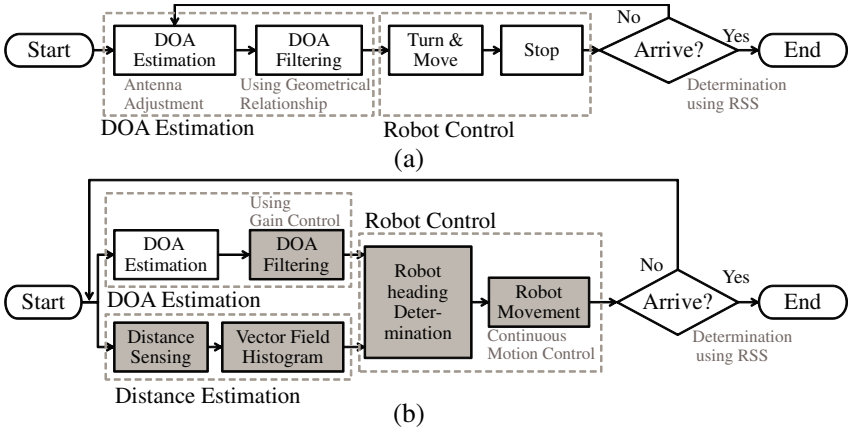

Figure 2. Flowchart of the robot docking. (a) Robot docking in the previous system. (b) Robot docking in the improved system.

are indicated by grey color. The distance estimation part is added for collision-free docking, and the robot control and DOA filtering parts are improved as shown in Fig. 2(b).

2.3. Fundamental of the DOA Estimation

The robot docking is based on the DOA estimation of RF signal transmitted from a target transponder. An accurate DOA estimation can be achieved by using an antenna array [21, 22]. However, the size

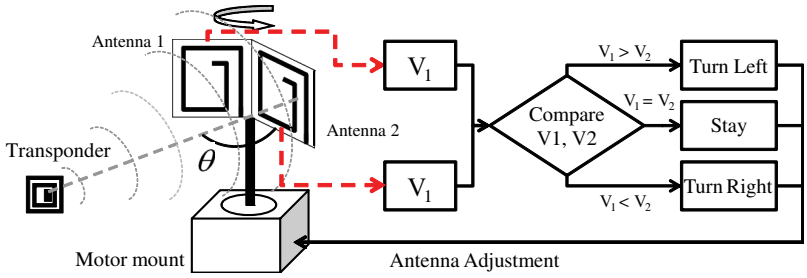

Figure 3. Overview of the dual directional antenna.

of the antenna array is too big, then it is hard to install it to the mobile robot.

Therefore, a dual directional antenna is employed to the RFID reader for estimating the DOA in this paper. The dual directional antenna is an antenna set consisting of perpendicularly positioned two identical spiral antennas, which have a size of $20 \times 20 \times 1$ mm and a half power beam-width of $89 \sim 92$ degrees. When an RF signal passes through the antenna with the angle of θ, the RSSs at each antenna draw a sine wave pattern [23–25] and has 90 degrees phase difference. Then the DOA of the transmitted signal can be estimated from their ratio difference as

$$\nu_{12} = V_1/V_2 = |\tan(\theta)| \rightarrow \theta = \tan^{-1}(\pm\nu_{12}), \tag{1}$$

where $\nu_{1,2}$ is the ratio, and V_1 and V_2 are the RSSs of each antenna.

However, since V_1 and V_2 include an off-set, which is changed by the environmental and system conditions, the estimated DOA from the ratio is not accurate enough, even though the off-set is measured and subtracted from RSS. However, there is a point which is not affected by the off-set. When the RF signal passes through the center between antennas 1 and 2, the ratio is always one regardless of the off-set. Therefore, the accurate DOA can be estimated by adjusting the antenna until the ratio becomes 1. Therefore, the antenna is mounted to the motor mount for adjusting its heading according to the ratio as shown in Fig. 3.

2.4. Robot Control

The robot navigates toward the target guided by the estimated DOA. In our previous work, the robot stops, turns toward the estimated DOA, and moves uniform interval as shown in the left of Fig. 4. However, such a stop, turn, and move control will cause unexpected but avoidable delay. In contrast, the robot can move to the expected

position by controlling each wheel's velocity. However, this will cause the robot to deviate from the DOA toward the target as shown in the right of Fig. 4. Therefore, we improve the robot control algorithm to make the robot keep the proper direction after movement.

Figure 5 shows the geometrical relationship when the robot moves from $(i-1)$th position to ith position, following two consecutive circular arcs by controlling each wheel's velocity. Two circles started from the $(i-1)$th and ith positions of the robot and directions of its heading are neighboring each other. Accordingly, the robot can reach the expected position with the proper heading as shown in Fig. 5.

The circular motion of robot can be calculated as follows. If we set a Cartesian coordinate originated from the $(i-1)$th robot position with the robot heading as x-axis as shown in Fig. 5, where d is the interval between robot positions, θ is the estimated DOA, and γ is the difference between the DOA and the expected robot heading after movement, respectively, the ith robot position can be written as $(d\cos\theta,\ d\sin\theta)$.

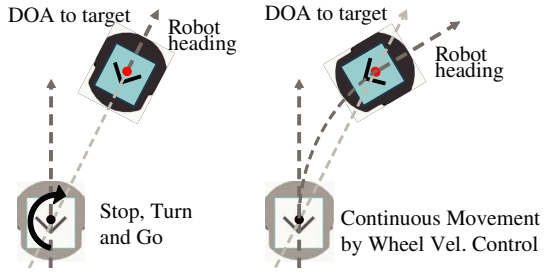

Figure 4. Change of the robot heading after movement.

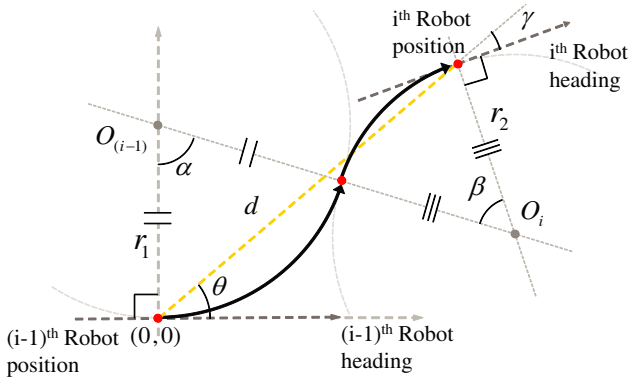

Figure 5. Schematic view of two-wheel steering control.

All angles in the equation are positive when it rotates counterclockwise. In the coordinate, the ith robot heading is $\theta + \gamma$, while the center O_i and O_{i-1} of the circle with radius r_i and r_{i-1} are given by

$$\begin{aligned} &O_{i-1} = (0, r_{i-1}), \\ &O_i = (d\cos\theta + r_i \sin(\theta+\gamma),\ d\sin\theta - r_i\cos(\theta+\gamma)). \end{aligned} \tag{2}$$

As the two circles are neighboring each other, the distance between the two centers of O_i and O_{i-1} is equal to the sum of r_{i-1} and r_i. We can obtain r_i as the function of r_{i-1} given by

$$r_i = \frac{d^2 - 2dr_{i-1}\sin\theta}{2(r_{i-1} - r_{i-1}\cos(\theta+\gamma) - d\sin\gamma)}. \tag{3}$$

Therefore, the robot path is determined by controlling the radius r_{i-1}. If the robot follows circular arcs with radius r_{i-1} and r_i whose central angles are α and β, the robot can arrive at the expected position with the proper heading. α and β are hereby written as

$$(\alpha, \beta) = \left(\cos^{-1}\left(\frac{r_{i-1} - d\sin\theta - r_i\cos(\theta+\gamma)}{r_{i-1} + r_i} \right),\ \alpha - (\theta+\gamma) \right). \tag{4}$$

3. FILTERING ALGORITHM

The robot employing the developed system can dock to the target transponder by following the estimated DOA using the robot control algorithm. The accuracy of the DOA estimation using a directional antenna was about $\pm 4^\circ$ in a free space [3]. However, as RF signals can be easily reflected, refracted, and scattered by the neighboring obstacles, multiple signals pass through the reader antenna [26, 27]. Thus, the total field Φ received by the antenna is the superposition of all those various RF waves and can be described as $\Phi_{total} = \Phi_{direct} + \sum_{i=1}^{n} \Phi^i_{non\text{-}direct}$. Then, the amplitude and the phase in the total field are changed according to the condition of the propagated waves as

$$\Phi_{total} = A_{sum}\sin(\theta + \eta_{sum}), \tag{5}$$

where A_{sum} is the amplitude difference, and η_{sum} is the phase difference in the superposed waves comparing with the direct wave. They cause an error in estimated RSS and DOA, respectively. In an isolated stable environment, it is possible to calculate the error using pre-measured RF signal map. Also, recent researches prove that the error in the dynamically changing environment can be calculated using the base stations [28]. However, since our work does not use any a *priori* environmental information and base stations, it is hard to use these methods.

To solve this problem, the filtering algorithm has been developed based on geometrical relationship between the estimated DOAs and moving distances of the robot in the authors' previous work [5]. The algorithm is very useful to find better direction toward the target even though the RF signal is distorted by the environmental effects. However, in order to use the algorithm, the robot should stop and wait until the antenna finds the direction which makes the ratio 1. Also, this algorithm does not work for the consecutive large errors in the estimated DOA.

The most simple method to reduce errors is averaging the estimated DOA. Even though there are large errors, the errors can become smaller by averaging. However, the error is reduced by as much as 1 over the number of averaged times regardless of the error size, also, the large error remains as far as it is included in the averaged DOA.

Therefore, a robust but efficient filtering algorithm is developed in this paper based on gain control to the difference between the previous and the current measurements. When a value v is estimated, the current value v_i at step i can be written as the summation of the previous estimation v_{i-1} and the difference between v_i and v_{i-1}. If there exists an error in the estimated value, the current value is bounded by v_i and v_{i-1}. Thus, the current value can be calculated as

$$v_i^* = v_{i-1}^* + g(v_i - v_{i-1}^*), \tag{6}$$

where v_i^* is the calculated value, v_i is the measured value, and g is the gain between the calculated and the measured values expressed as

$$\begin{aligned} g &= \frac{\mathrm{VAR}(\delta v_j^*)}{\mathrm{VAR}(\delta v_j^*, \delta v_i)}, \quad j = 2 \text{ to } i-1 \\ \delta v_j^* &= v_j^* - v_{j-1}^*, \quad \delta v_i = v_i - v_{i-1}^* \end{aligned} \tag{7}$$

where $\mathrm{VAR}(\delta v_j^*)$ is variance of δv_j^*, and $\mathrm{VAR}(\delta v_j^*, \delta v_i)$ is variance including δv_i. The gain is changed by reflecting the change of the estimated value. If the change between the current and previous estimations is almost the same as the change between the previous and pre-previous estimations, the denominator and numerator are almost the same, and g increases. On the contrary, if the current change is very different from the previous one, g is reduced, then the current change is less reflected. Note that the number of data included in the variance can affect g. If the number increases, the effect of δv_i on g reduces. However, since the robot arrives at target position around 10 to 20 steps in our application, the number of data in the variance is not considered.

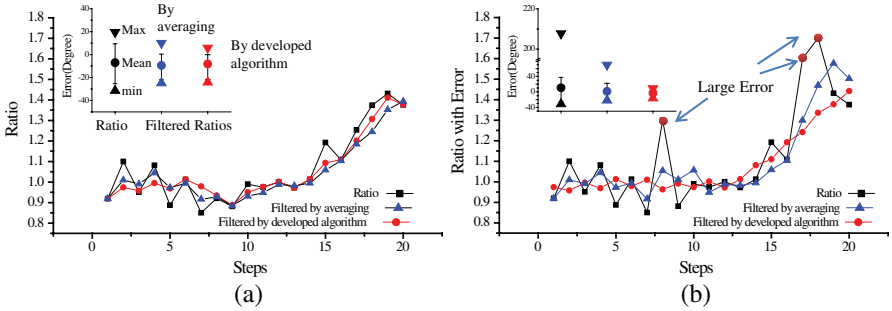

Figure 6. Estimated ratio with filtered ratio by the developed algorithm. (a) Estimated ratio. (b) Ratio with the large error.

Figure 6 shows how the gain works. The ratio pattern is obtained when a transponder is moved 2 meters backward with the direction unchanged, and moved subsequently 2 meters to the right in our hallway environment. The black solid line with square dots in the graph shows the non-filtered data while the blue solid line with triangle dots and red solid line with round dots show the filtered data by adjusted averaging of 3 steps and the developed filter based on gain control, respectively. The statistical results of the error between the accurate DOA and the estimated DOA from the ratio are inserted.

The left graph shows the results of original estimation. As shown in the graph, the ratios are smoothened in both cases, and the errors decrease. In order to verify the developed algorithm, arbitrary large errors are added to the estimated ratio and we perform test again. The developed algorithm shows better performance than the adjusted average even though there are consecutive large errors as shown in the right of figure.

3.1. Collision-avoidance Based on Vector Field Histogram

The transmitted DOA of RF signal does not always allow the robot to move toward the target. The permeability of RF signal is very useful to identify the object without the need for the line of sight, but it is not always advantageous for the robot navigation. The robot may fail to dock to the target due to the collision with the obstacles which allow an RF signal to pass through. To solve this problem, distance measuring sensors are fused and a collision-avoidance algorithm is developed in this paper.

Among several collision-avoidance techniques, the vector field histogram technique is chosen, because the technique enables the robot

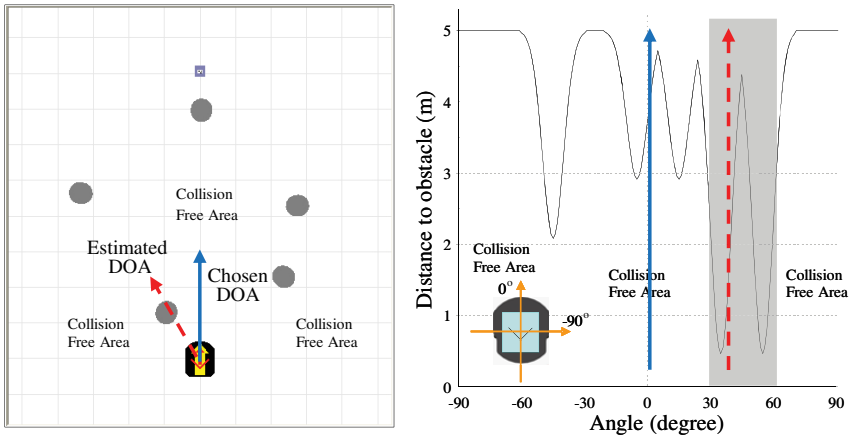

Figure 7. Determination of moving direction. (a) Robot surrounded by many obstacles. (b) Finding nearest collision-free space from the estimated DOA.

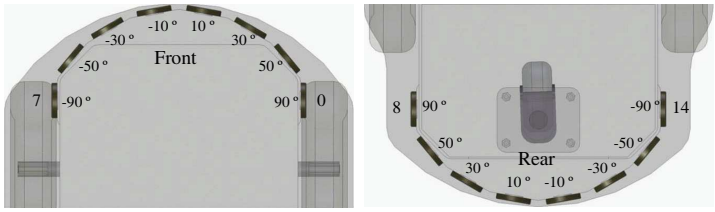

Figure 8. Alignment of the sonar sensors in pioneer 3DX.

to react to the rapid change of the environmental conditions using one-dimensional histogram reflecting the distance to the neighboring obstcles without any *priori* map. Fig. 7 shows the basic concept of the collision-avoidance using the vector field histogram. The left of Fig. 7 shows the environmental conditions while the right shows the vector field histogram using the measured distances. When the robot faces an obstacle in the estimated direction, the robot can find the bypass route toward the goal without any collision by choosing the nearest collision-free direction from the estimated DOA. Since the RFID system gives the DOA to the goal continuously, the local collision-avoidance technique is really effective.

For the distance measurement, the sonar ring installed in Pioneer 3DX is used in this work. A total of 8 front and 8 rear sonar sensors are installed with non-uniform intervals as shown in Fig. 8. A valid

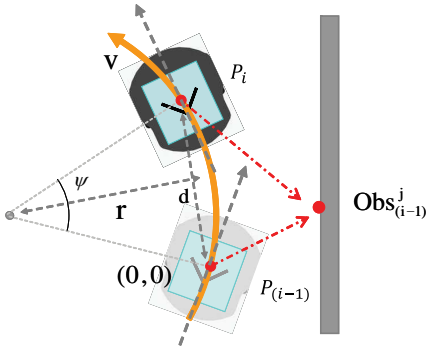

Figure 9. Geometrical relationship between the sensed obstacle and the robot.

distance of the sensor is up to 5 meters within the cone angle about $\pm 12^{\circ}$, which is determined empirically.

However, since the sonar sensors are fixed, there is non-detected area by the sonar sensors. In order not to miss neighboring obstacles within the area, the distance measuring information is updated while robot moves as follows. Fig. 9 shows the change of the obstacle position in the local coordinate of the moving robot. When a robot moves from the position P_{i-1} to P_i following the arc with a radius of r with uniform velocity of v, the central angle ψ after time t can be calculated as $\psi = \frac{v}{r}t$, which is the same as the change of the robot heading direction. The moving interval d is determined using the radius and the central angle as $2r \sin \frac{\psi}{2}$. Therefore, the current position P_i in the coordinate originated at P_{i-1} can be calculated as

$$P_i = (r \sin \psi,\ r - rcos\psi). \tag{8}$$

If the object position sensed by jth sensor at the position P_{i-1} is (a, b), the position at P_i can be calculated through linear and angular transformations as

$$Obs_i^j = (a \cos \psi + b \sin \psi - r \sin \psi,\ -a \sin \psi + b \cos \psi - r \cos \psi) \tag{9}$$

Then the previously observed obstacles can be updated by including Obs_i^j to the current estimation. However, the error in previous estimation remains and it becomes larger by the odometry error of the robot. In consideration of this problem, the estimated values are updated in the Gaussian form as follows. When an obstacle is sensed with a distance of d and an angle of θ, the direction can be normalized as

$$f(x) = ge^{-\frac{(x-\theta)^2}{2c^2}}, \tag{10}$$

where g is the height of the Gaussian peak with the full width half maximum c. If g decreases while c increases, the Gaussian curve is lowered and spread. g is set as 1 for the first estimation. Also, c is $\frac{24}{2\sqrt{2\ln 2}}$, because the coverage of the sonar sensor is $\pm 12°$. The direction of the obstacle is chosen from the Gaussian curve whose amplitude is over 0.5. When the robot moves, the estimated obstacle is transformed. However, as there may exist errors in the measured distance and robot odometry, the estimated angle and distance become inaccurate. Thus, we reduce g and increase c after transformation and add the spread curve to the current estimation. If the estimation is inaccurate, it will disappear by this process. g is lowered and c is increased with the interval of 0.2.

Figure 10 shows how this method works. When a robot senses an obstacle that is 3 meters away by the sonar positioned at -50 degrees in front, the sensed direction is spread in Gaussian form and the vector field is generated using the sensed direction over 0.5 as drawn in the Fig. 10(a). After then, the robot turns 15 degrees counterclockwise and senses another obstacle as shown in Fig. 10(b). The direction to the previously-sensed obstacle is moved reflecting the robot's rotation. However, if the previously-sensed obstacle is not sensed again, the amplitude is decreased and spread. Fig. 10(c) shows the sensed directions and the vector field after two steps from Fig. 10(b). Since the obstacle 1 is not sensed again, the direction information will be erased. However, as the obstacle 2 is sensed continuously, the sensed information is added and remains in the vector field histogram.

4. EXPERIMENT RESULTS

4.1. Simulation Results

To test the developed technique, the DOA based robot docking is simulated using the in-house simulator. The RF signal propagation error is included using a ray-tracing model [26]. As the purpose of the simulation is to verify the effectiveness of the developed system, it is not necessary to include all complex factors from the real environment. Therefore, the simulation condition is simplified as follows:

- The environment is an isolated 5.5×6 m square space.
- RF signal is propagated from a transponder to all directions.
- RF signal is reflected from obstacles, which are cylinder shape with the same physical properties.
- There is no error in distance measurement.
- Intrinsic error in the estimated DOA is under $\pm 4°$.

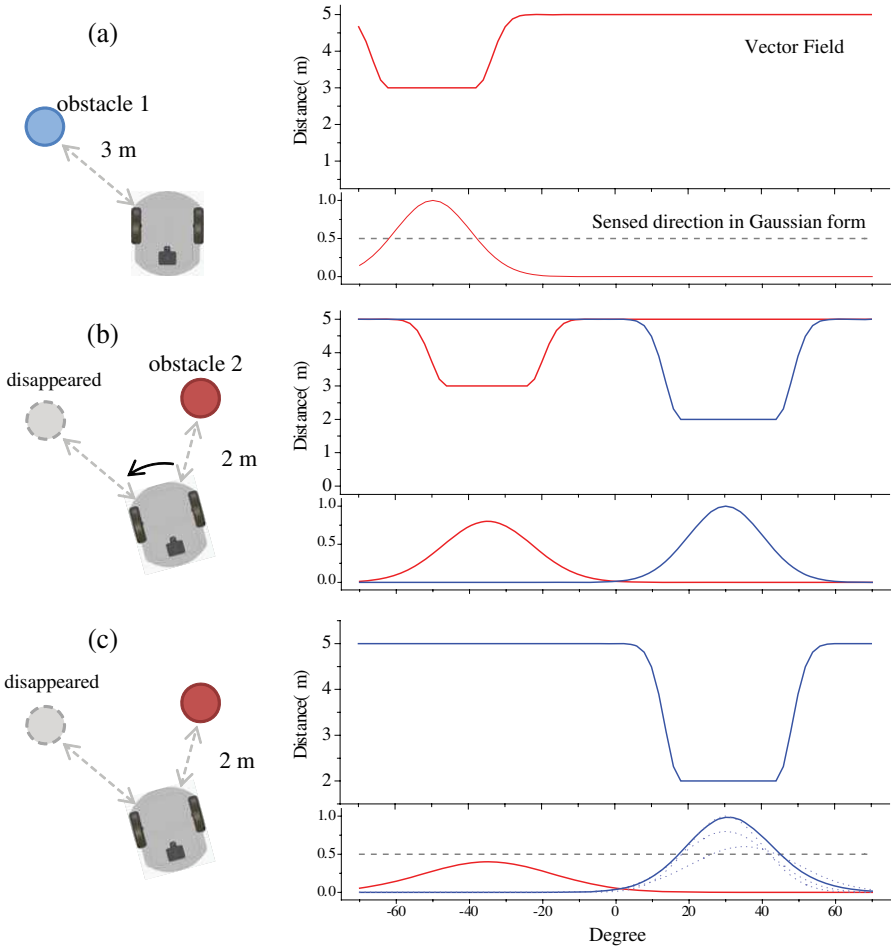

Figure 10. Vector field histogram generated using the merged sonar data.

- No odometric error exists in robot movement.

In the environment, the robot moves to the target transponder according to the following steps.

(i) The robot scans the transmitting signal from $-90°$ to $90°$.

(ii) The function about the relationship between the ratio and DOA is made from the ratio pattern acquired from above measurement.

(iii) The robot moves toward the estimated DOA and adjusts its heading following the filtered DOA with an uniform interval.

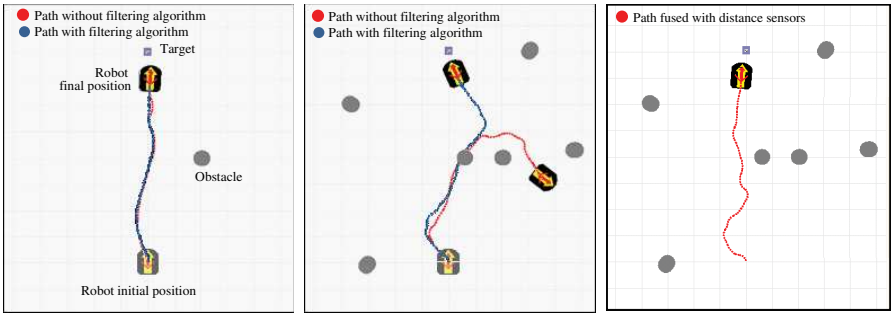

Figure 11. Simulation results of robot docking, (a)in space with an obstacle, (b) in space with randomly positioned obstacles, (c) avoiding collision using vector field histogram.

(iv) The robot stops when it enters the target area, which is determined by the signal strength.

Figure 11 shows one of the simulation results, which demonstrates the robustness of the developed algorithm in various conditions. Figs. 11(a) and (b) show the robot docking with and without the DOA filtering algorithm indicated by red line and blue line, respectively. The results clearly show that the robot can dock to the target position even though the RF signal is terribly distorted by the cluttered obstacles. However, the robot collides with an obstacle as shown in Fig. 11(b). In regards to this problem, the distance information to the neighboring obstacles are added and the developed collision-free robot docking algorithm is tested under the same condition of Fig. 11(b). It is obviously that the robot finds the collision-free area and can arrive at the target position eventually as shown in Fig. 11(c).Based on the simulation results, we perform the experiment using a mobile robot Pioneer 3DX under various environmental conditions and situations. The detailed results are described in the following section.

4.2. Real Robot Experimental Results

Figure 12 shows a snapshot of the experimental scene and its graphical representation of our experimental room conditions. Paper boxes are used as the obstacles that block the robot's moving path but allow RF signal to pass through. A transponder is attached on the top of a paper box as a target. In addition, chairs and a human are positioned to make RF signal distortion that causes a great fluctuation in the estimated DOA.

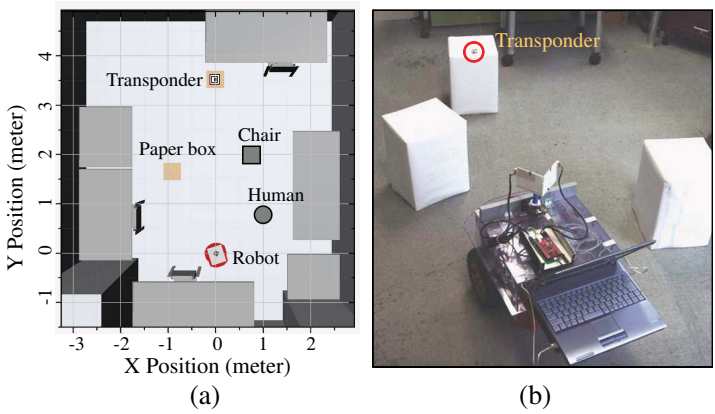

(a) (b)

Figure 12. Environmental experiment. (a) Virtual environment for displaying the results. (b) Snapshot of real environment.

4.2.1. Robot Docking with and without the Filtering Algorithm

Robot docking experiment is performed for the target transponder located at the position of $(0, 3.5)$ m in Cartesian coordinate originated from the initial position of the robot. The robot moves to the target transponder following same steps of the simulation. If the robot can not arrive at the target position within 2 minutes, it is included in the failure.

Figure 13 shows the results obtained from two different conditions. The grey squares indicate the initial positions of the robot and the transponder. The black and red dashed lines are the paths that the robot navigates while the black circles and red diamonds are final positions of the robot. When there is no neighboring obstacle, the robot can arrive at the transponder position in both cases as shown as in the left of Fig. 13. By placing obstacles which can affect the RF signal propagation, the DOA estimation error increases then the robot loses the direction toward the target and it knocks into the desk as shown in the right of Fig. 13. However,the error is reduced by using the filtering algorithm then the robot can arrive at the target position.

4.2.2. Collision-free Robot Docking Using Vector Field Histogram

The left of Fig. 14 shows the vector field histogram using estimated distances to neighboring obstacles in Polar coordinate. Four paper boxes are positioned near the robot. As shown in the figure, the obstacles are identified well by updating the estimated distance data

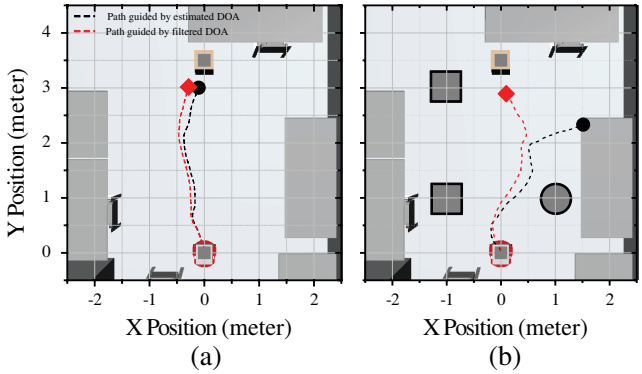

Figure 13. Robot docking under various conditions (a) without any neighboring obstacles (b) with neighboring obstacles of metallic objects and a human.

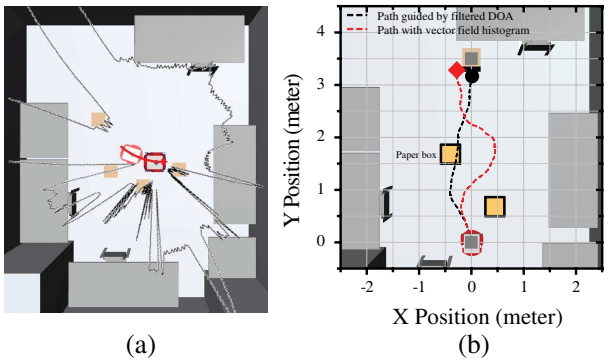

Figure 14. Collision-free robot docking (a) Vector field histogram from the distance estimation by sonar sensor array (b) Results of robot docking.

while the robot moves. From the vector field, the robot can find collision-free path to the target as shown in the right of Fig. 14. When the robot follows the originally-estimated DOA, the robot collides with the boxes. In contrast, by using the collision-avoidance algorithm, the robot can effectively avoid the boxes and arrive at the target position.

Table 1 shows the statistics of the experimental results of 50 trials in the simulation and 10 trials in the real robot experiment. The SR is the success rate, and T is the average time spent for the robot docking. The robot docks to the target transponder in the environment where 1 to 5 paper boxes are randomly positioned. As shown in the table,

Table 1. Statistics of the robot docking experiments.

Results	Simulation (50 trials)		Experiment (10 Trials)			
No. of	Without Sensor	With Sensor	Without Sensor		With Sensor	
Obstacles	SR (%)	SR (%)	SR (%)	T (s)	SR (%)	T (s)
0	96	94	90	26	100	28
1	76	90	70	32	80	37
3	50	84	30	38	80	48
5	36	66	10	35	60	57

the success rate increases when the robot uses the distance measuring sensors and the collision-avoidance algorithm. Since the robot should move more distance, collision-free docking takes more time as shown in the table.

The success rate decreases as the number of obstacles increases then it is not so high enough when there are many obstacles in a small space. This is caused by two reasons as follows. Firstly, the collision-avoidance performance depends on the number and property of the distance measuring sensor. Since the used sonar sensor senses more widely than the occupied area by obstacles then the robot sometimes can not pass through the space between two obstacles even though there is enough gap. Secondly, the vector field histogram does not requires a *priori* map and is robust to the unforeseen situations but weak to the local minima. If the collision-free path in the previous estimation is finally blocked, the robot cannot escape from the blocked area. In order to solve these problems, more accurate distance estimation sensors such as laser range finder and an algorithm for escaping from the local minima are required to the developed system.

5. CONCLUSIONS

The target identification and docking mobile robot system employing DOA estimation RFID is presented in this paper. The sensors for distance measurement are adopted for the collision-free mobile robot docking in the obstacles-cluttered indoor environment. Also, the DOA estimation error correction algorithm which is available to the improved robot control algorithm is incorporated with the proposed system. The experimental results prove that the collision-free robot docking becomes available without a *priori* map and target position. However, the success rate does not reach a satisfactory level to be used in commercial mobile robots. Therefore, our future effort will

be devoted to improve the robot docking algorithm including the function to escape from the local minima problem as well as develop a location sensing technique with multiple transponders using the data transmission in the *ad hoc* network of RFID transponders.

ACKNOWLEDGMENT

The research was supported by the Converging Research Center Program through the Ministry of Education, Science and Technology (2010K001051).

REFERENCES

1. Chong, N. Y., H. Hongu, K. Ohba, S. Hirai, and K. Tanie, "A distributed knowledge network for real world robot applications," *Proc. IEEE/RSJ Int. Conf. on Intelligent Robots and Systems*, 187–192, 2004.
2. Holmquist, L. E., H. W. Gellersen, G. Kortuem, S. Antifakos, F. Michahelles, B. Schiele, M. Beigl, and R. Maze, "Building intelligent environments with smart-its," *IEEE Computer Graphics and Applications*, Vol. 24, No. 1, 56–64, 2004.
3. Kim, M. and N. Y. Chong, "RFID-based mobile robot guidance to a stationary target," *Mechatronics*, Vol. 11, No. 4–5, 217–229, 2007.
4. Kim, M., H. W. Kim, and N. Y. Chong, "Automated robot docking using direction sensing RFID," *Proc. IEEE Int. Conf. on Robotics and Automation*, 4588–4593, 2007
5. Kim, M. and N. Y. Chong, "Direction sensing RFID reader for mobile robot navigation," *IEEE Transactions on Automation Science and Engineering*, Vol. 6, 44–54, 2009.
6. Yuen, D. C. K. and B. A. MacDonald, "Vision-based localization algorithm based on landmark matching, triangulation, reconstruction, and comparison," *IEEE Transactions on Robotics*, 217–226, 2005.
7. Se, S., D. G. Lowe, and J. J. Little, "Vision based global localization and mapping for mobile robots," *IEEE Transactions on Robotics*, 364–375, 2005.
8. Hightower, J. and G. Borriello, "Location systems for ubiquitous computing," *IEEE Computer Magazine*, Vol. 34, 57–66, 2001.
9. Smith, A., H. Balakrishnan, M. Goraczko, and N. Priyantha, "Tracking moving devices with the cricket location system," *Proc.*

2nd Int. Conf. on Mobile Systems, Applications, and Services, 190–202, 2004.

10. Balh, P. and V. N. Padmanabhan, "Radar: An in-building RF-based user location and tracking system," *Proc. of IEEE INFOCOM*, 775–784, 2000.
11. Ni, L. M., Y. Liu, Y. C. Lau, and A. P. Patil, "LANDMARC: Indoor location sensing using active RFID," *ACM Wireless Networks*, Vol. 10, No. 6, 701–710, 2004.
12. Tan, K. G., A. W. Reza, and C.-P. Tan, "Objects tracking utilizing square grid RFID reader antenna network," *Journal of Electromagnetic Waves and Applications*, Vol. 22, No. 1, 27–38, 2008.
13. Bahillo, A., S. Mazuelas, R. M. Lorenzo, P. Fernández, J. Prieto, and E. J. Abril, "Indoor location based on IEEE 802.11 round-trip time measurements with two-step NLOS mitigation," *Progress In Electromagnetics Research B*, Vol. 15, 285–306, 2009.
14. Reza, A. W., S. M. Pillai, K. Dimyati, and T. K. Geok, "A novel positioning system utilizing zigzag mobility pattern," *Progress In Electromagnetics Research*, Vol. 106, 263–278, 2010.
15. Hahnel, D., W. Burgard, D. Fox, K. Fishkin, and M. Philipose, "Mapping and localization with RFID technology," *Proc. IEEE Int. Conf. on Robotics and Automation*, 1015–1020, 2004.
16. Niculescu, D. and B. Nath, "Ad hoc positioning system (APS) using AOA," *Proc. of IEEE INFOCOM*, 1734–1743, 2003.
17. Stefano, G. D. and A. Petricola, "A distributed AOA based localization algorithm for wireless sensor networks," *Journal of Computers*, Vol. 3, No. 4, 2008.
18. Seow, C. K. and S. Y. Tan, "Localization of omni-directional mobile device in multipath environments," *Progress In Electromagnetics Research*, Vol. 85, 323–348, 2008.
19. Tayebi, A., J. Gomez, F. Saez de Adana, and O. Gutierrez, "The application of ray-tracing to mobile localization using the direction of arrival and received signal strength in multipath indoor environments," *Progress In Electromagnetic Research*, Vol. 91, 1–15, 2009.
20. Song, H. B., H. G. Wang, K. Hong, and L. Wang, "A novel source localizations scheme based on unitary esprit and city electronic maps in urban environments," *Progress In Electromagnetic Research*, Vol. 94, 243–262, 2009.
21. Lie, J. P., B. P. Ng, and C. M. See, "Multiple UWB emitters DOA estimation employing time hopping spread spectrum," *Progress In*

Electromagnetic Research, Vol. 78, 83–101, 2008.

22. Lizzi, L., F. Viani, M. Benedetti, P. Rocca, and A. Massa, "The M-DSO-esprit method for maximum likelihood DOA estimation," *Progress In Electromagnetic Research*, Vol. 80, 477–497, 2008.
23. Pozar, D. M., *Microwave and RF Wireless Systems*, Wiley Text Books, 2000.
24. Stutzman, W. L. and G. A. Thiele, *Antenna Theory and Design*, John Wiley & Sons Ltd., 1999.
25. Balantis, C. A., *Antenna Theory: Analysis and Design*, Wiley Text Books, 1996.
26. Alves, F. A., M. R. L. Albuquerque, S. G. Silva, and A. G. d'Assuncao, "Efficient ray-tracing method for indoor propagation prediction," *Proc. SBMO/IEEE MTT-S Int. Conf. on Microwave and Optoelectronics*, 435–438, 2005.
27. Tsang, L. and J. A. Kong, *Scatterning of Electromagnetic Waves: Advanced Topics*, John Wiley & Sons Ltd., 2001.
28. De Moraes, L. F. M. and B. A. A. Nunes, "Calibration-free WLAN location system based on dynamic mapping of signal strength," *ACM MOBIWAC*, 92–99, 2006.